Cosmic Masers: Proper Motion toward the Next-Generation Large Projects
Proceedings IAU Symposium No. 380, 2024
T. Hirota, H. Imai, K. Menten, & Y. Pihlström, eds.
doi:10.1017/S1743921323002028

Galactic astrometry with Gaia

Carme Jordi[1,2,3,4]

[1]Institut de Ciències del Cosmos (ICCUB), Universitat de Barcelona (UB), Martí i Franquès 1, E-08028 Barcelona, Spain. email: carme@fqa.ub.edu

[2]Departament de Física Quàntica i Astrofísica (FQA), Universitat de Barcelona (UB), Martí i Franquès 1, E-08028 Barcelona, Spain

[3]Institut d'Estudis Espacials de Catalunya (IEEC), c. Gran Capità, 2-4, E-08034 Barcelona, Spain

[4]Institut dEstudis Catalans, c. Carme 47, E-08001, Barcelona, Spain

Abstract. *Gaia* space mission of the European Space Agency was launched at the end of 2013 and will continue operations until 2025. The published data releases revolutionize the view of the Milky Way galaxy and beyond thanks to its unprecedented astrometry, photometry and spectroscopy. The paper reviews the products of the last data release of the Gaia mission and some of the scientific impacts of the data. We also discuss the future perspectives of Galaxy astrometry from space.

Keywords. Galaxy, astrometry, photometry, spectroscopy

1. Introduction

Gaia space mission (Gaia Collaboration, Prusti *et al.* 2016) by the European Space Agency was launched to space in December 2013. Routine operations are going on smoothly since July 2014 at an average rate of 70 million source observations per day. The nominal mission of 5 years ended in July 2019 and the mission is currently in an extended operation period that will last until the exhaustion of cold gas around the first quarter of 2025.

The satellite is in orbit around the Earth-Sun Lagrange point L2 at 1.5 million kilometers from Earth. It holds two telescopes each one pointing to a different field-of-view. Both field-of-views are separated a large basic angle of 106.5 degrees. The rotation around the own spin axis, the precession of this spin axis around the direction Earth-Sun and the yearly rotation around the Sun makes that the two telescopes scan the full-sky about every six months.

The focal plane is equipped with 106 CCD cameras operating in Time-Delay-Integration mode with about 1 Giga pixels in total, the largest camera sent to space ever. These cameras serve different purposes and instruments: on board detection of point like sources (mainly stars, but also small bodies of our Solar System, far galaxies and quasars), astrometry, photometry, low and medium spectroscopy, monitoring of the basic angle and wave front sensors.

The repeated observations over time of the same objects allow the determination of positions, brightness, spectral energy distribution and radial velocity as well as their variations thus proper motions, parallaxes, changes in brightness, colours and radial velocities. The unprecedented precision of the data and the volume of the data makes the mission *Gaia* a revolution for many fields of astrophysics, from the Milky Way Galaxy

itself, to stellar physics, exoplanetary science, extragalactic astronomy and general relativity.

So far, the *Gaia* Data Processing and Analysis Consortium (DPAC) has published three releases: DR1 (Gaia Collaboration, Brown *et al.* 2016), DR2 (Gaia Collaboration, Brown *et al.* 2018) and DR3 (Gaia Collaboration, Vallenari *et al.* 2023), which includes its early release EDR3 (Gaia Collaboration, Brown *et al.* 2021). This paper reviews the content of the last data release and highlights some of the main results.

After the present introduction, Sec. 2 describes the main products of the third *Gaia* release, Sec. 3 describes some results of performance verification papers and from community at large, and Sec. 4 describes the steps forward the future, including the next generation of future space astrometry.

2. (E)DR3 content

Gaia DR3 (Gaia Collaboration, Vallenari *et al.* 2023) published in June 2022 includes data for about 1.8 billion sources, mainly stars in our Milky Way galaxy. Astrometry (positions, proper motions and parallaxes) and photometry (apparent brightness in white band G and colour blue-red $G_{\rm BP} - G_{\rm RP}$) for about 1.5 million sources were advanced in the early release in December 2020 (Gaia Collaboration, Brown *et al.* 2021). Therefore, DR3 extends DR2 in terms of number of variable stars, radial velocities, astrophysical parameters and Solar System objects and completes EDR3 with novel products published for the first time like rotational velocities, chemical abundances, multiple systems and galaxies and quasars. The release is also complemented by the publication light curves for all sources in a field-of-view of one degree centered on Andromeda's galaxy. All data is accessible at the *Gaia* archive site https://gea.esac.esa.int/archive/.

2.1. *Astrometry*

The astrometric content is fully described in Lindegren *et al.* (2021) and the summary can be found in the EDR3 publication (Gaia Collaboration, Brown *et al.* 2021). The uncertainties of positions, proper motions and parallaxes have decreased both by the longer time baseline of the observations (from 22 months in DR2 to 34 months in DR3) and for the improvements introduced in all steps of the data processing pipeline by DPAC. Systematic errors still dominate the bright regime (to about $G = 13$), while the faint regime is dominated by the photon-noise statistics (see Fig. 7 in Lindegren *et al.* (2021)).

Worth to notice that systematic errors as mapped through quasars parallaxes and proper motions are much smaller than those in DR2, and both at large and small angular scales as shown in Fig. 1. The later have been derived by analysing the parallaxes and proper motions of stars in the Large Magellanic Cloud area. The global parallax zero point is -17 μas and the rms angular variations are 26 μas and 33 μas yr^{-1} for parallaxes and proper motions, respectively. The dependencies on magnitude, colour and sky position can be calculated using the code in https://gitlab.com/icc-ub/public/gaiadr3_zeropoint.

2.2. *Medium resolution spectroscopy*

One of jewels of DR3 is its spectroscopic content. The medium resolution spectrograph (RVS) has provided the third component of the velocity, the radial velocity, for 33 million stars, the largest catalogue of radial velocities ever (Katz *et al.* 2023). This is complemented with 3.5 millions of rotational velocities, 2.5 millions of chemical abundance determinations and with 1 million spectra, more spectra than those collected over

https://doi.org/10.1017/S1743921323002028 Published online by Cambridge University Press

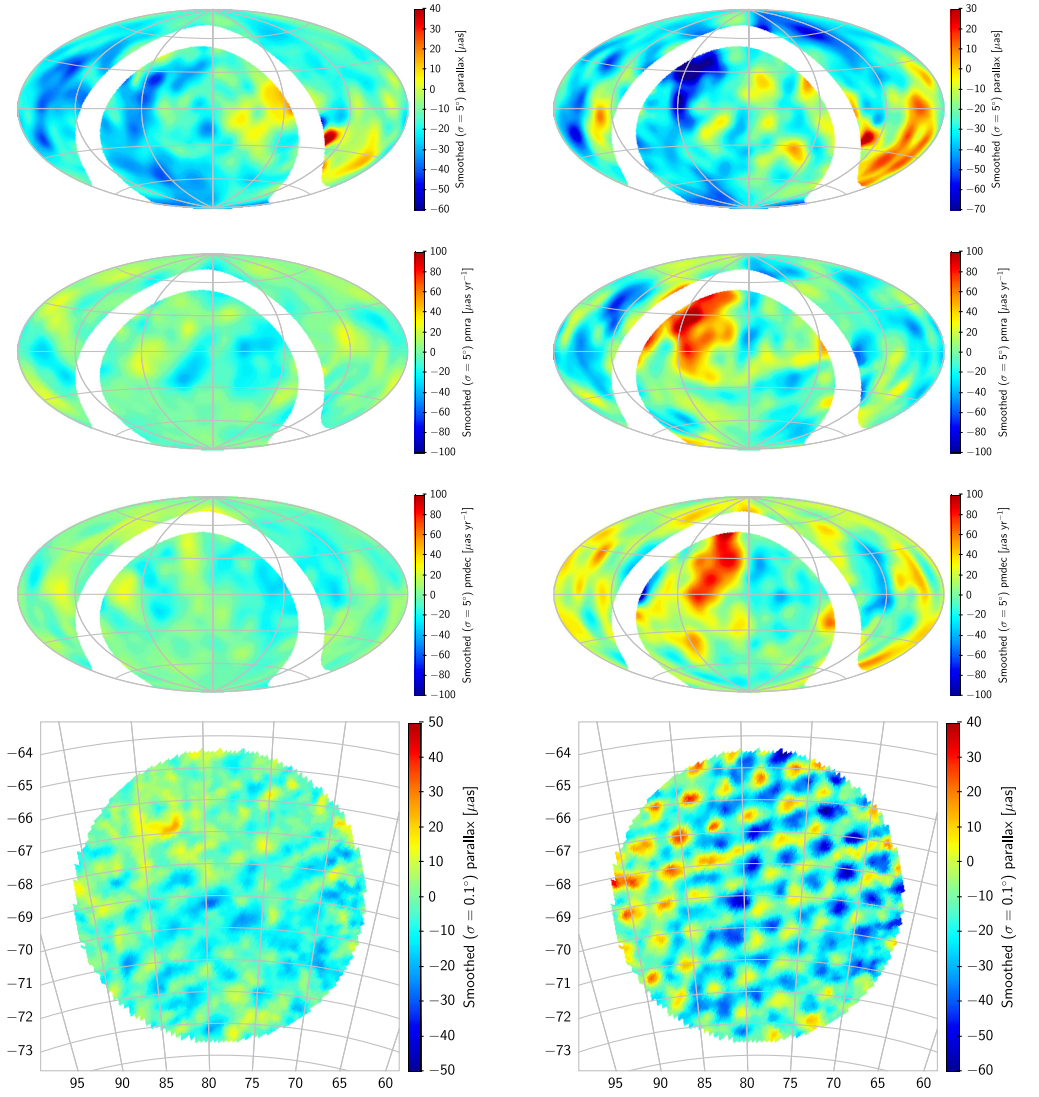

Figure 1. Figures 13 and 14 of Lindegren *et al.* (2021). The three top panels show the all sky smoothed maps of quasars parallaxes and proper motions, while the low panels show the smoothed maps of parallaxes in the Large Magellanic Cloud area. Left panels are for EDR3/DR3 and right panels for DR2.

all centuries. The sample of stars cover the range of $T_{\rm eff} \in [3100, 14500]$ K for the bright stars ($G_{\rm rvs} \leq 12$) and [3100, 6750] K for the fainter stars, reaching a few kilo-parsecs beyond the Galactic centre in the disc and up to about $10 - 15$ kpc vertically into the inner halo. The median uncertainties of the radial velocities are of 1.3 km s^{-1} at $G_{\rm rvs} = 12$ and 6.4 km s^{-1} at $G_{\rm rvs} = 14$. The radial velocity scale is in satisfactory agreement with APOGEE, GALAH, GES and RAVE, with systematic differences that mostly do not exceed a few hundreds m s^{-1}. The velocity zero point has a small systematic shift starting around $G_{\rm rvs} = 11$ and reaching about 400 m s^{-1} at $G_{\rm rvs} = 14$. From the RVS spectra rotational velocities, astrophysical parameters and chemical abundances have also been derived (see Sec. 3), as well as radial velocity variables have been identified.

https://doi.org/10.1017/S1743921323002028 Published online by Cambridge University Press

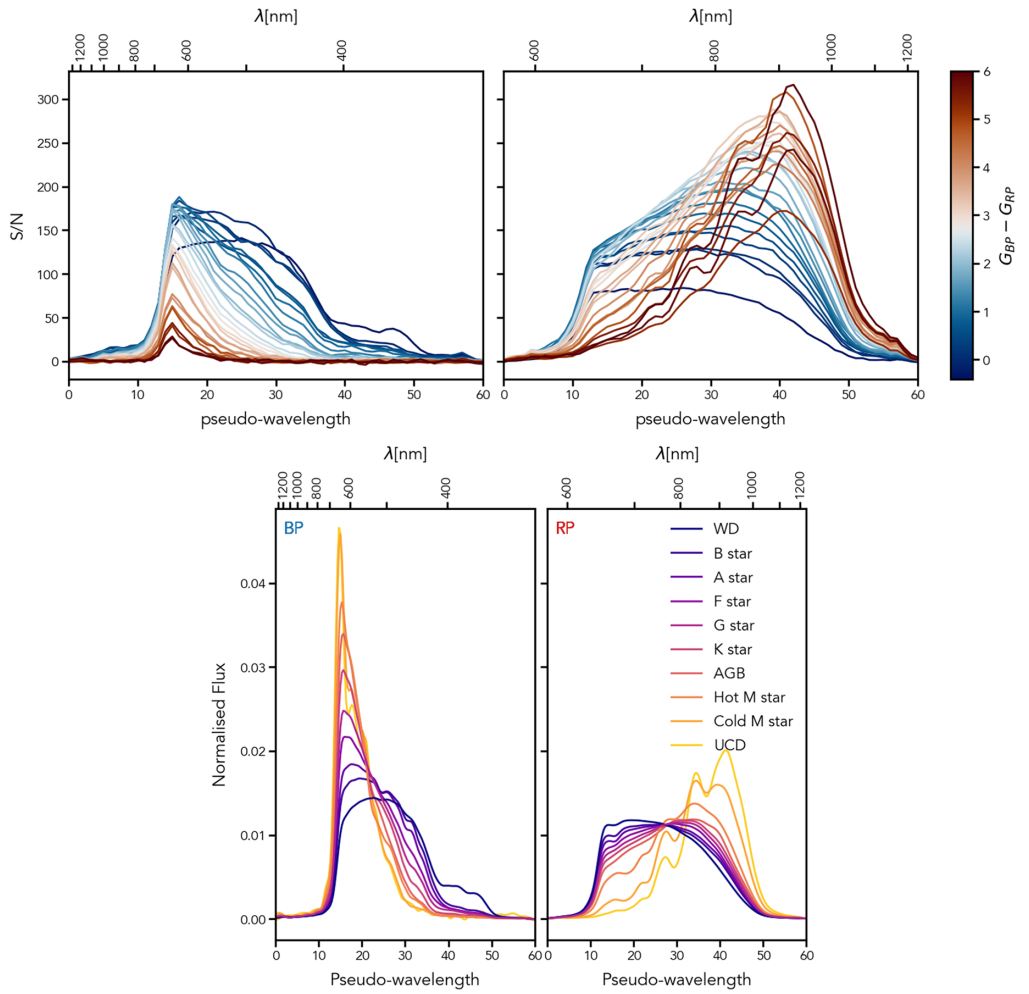

Figure 2. Figures 24 (top) and 26 (bottom) from De Angeli *et al.* (2023) showing the signal-to-noise ratio for stars of $G = 16$ and different colors $G_{\rm BP} - G_{\rm RP}$ and the normalised internal mean spectra for different types of stars. BP are shown in the left and RP in the right.

2.3. *Low resolution spectroscopy*

Low-resolution spectroscopy is acquired for every source transiting the *Gaia* focal plane. Spectral energy distribution (SED) are obtained in the blue (BP) and red (RP) globally covering the wavelength range [330, 1050] nm. These SEDs are the basis of the object classification into stars, quasars, galaxies and so on, and the determination of the astrophysical parameters (see Sec. 3). Bottom panel of Fig. 2 shows the normalized SEDs with different shapes for different types of stars. Top panel of Fig. 2 shows the signal-to-noise ratio for stars of $G = 16$ and different colors $G_{\rm BP} - G_{\rm RP}$. As expected, this signal-to-noise ratio depends on the wavelength, the magnitude and the colour of the objects, with sources around $G = 15$ having signal-to-noise above 100 in some wavelength ranges and reaching 1000 in the central part of the RP wavelength range for sources with magnitudes $9 < G < 12$ (De Angeli *et al.* 2023). The SEDs are provided internally and externally calibrated using a set of spectrophotometric standard stars. The spectra are represented by a set of coefficients and basis functions, in such a way that the analysis of the coefficients suffices for the classification and the detection of spectral features. In

https://doi.org/10.1017/S1743921323002028 Published online by Cambridge University Press

addition, the tool `GaiaXPy` is also provided to represent the spectra in traditional form or to compute synthetic photometry from the SEDs. DR3 includes about 220 SEDs most of them for objects brighter than $G = 17.65$.

2.4. *Derived products*

All the above data, astrometry, photometry and spectroscopy, are the basis for the multiple derived products included in DR3: (a) the classification of 1.5 billion sources into stars, galaxies, quasars and so on, (b) physical parameter determination for 470 million stars (temperatures, surface gravity, absorption, luminosities and radii and masses and ages for 128 million stars, (c) the analysis of 10 million light curves including more variability types than in DR2, (d) properties of 813 000 binary systems including binaries with compact objects, detection of 297 exoplanets, of which 114 are new candidates, (e) astrophysical parameters for 470 millions of stars from low resolution spectroscopy and for 5.6 million stars from medium resolution spectroscopy, (f) chemical abundances for 2.5 million stars from medium resolution spectroscopy, (g) data for 3 million galaxies and 2 million quasars, (h) orbits for 156 000 asteroids, BP/RP reflectance spectra of 60 000 asteroids. See all papers in https://www.cosmos.esa.int/web/gaia/dr3-papers.

3. Results

The richness of results based on *Gaia* data releases is enormous and impossible to review here. Only some of the results of the performance verification papers and some of the results related with archaeology of the Galaxy are described in the following. The selection is incomplete and biased by the author.

3.1. *Milky Way structure and dynamics*

The dynamical perturbations of the thin and thick discs due to accretion of galaxies by the Milky Way were soon realized after the publication of DR2. The perturbations of the orbits of the stars in the solar neighbourhood due to the pass of the Sagittarius dwarf galaxy are still noticeable in the present Antoja *et al.* (2018), and a set of stars in retrograde orbits confirm their extragalactic origin and has been called Gaia-Enceladus galaxy Helmi *et al.* (2018). The triggered star formation in bursts due to the subsequent passes of the Sagittarius dwarf galaxy was also detected through the analysis of stellar populations Ruiz-Lara *et al.* (2020). EDR3 provided new insights of these and other mergers in terms of dynamical perturbations and stellar populations (Gaia Collaboration, Antoja *et al.* 2021; Ramos *et al.* 2022).

The map of radial velocities (Fig. 3 left) shows the pattern of approaching and receding stars with respect to the Solar System due to the Galactic rotation and Solar System motion with respect to the local standard of rest. The 3D position and 3D motion information has been used to map the spiral structure associated with star formation $4 - 5$ kpc from the Sun by using 2800 Classical Cepheids younger than 200 million years, which show spiral features extending as far as 10 kpc from the Sun in the outer disc (Gaia Collaboration, Drimmel *et al.* 2021). The velocity field has been mapped through red giant branch stars with radial velocities as far as 8 kpc from the Sun, including the inner disc. The spiral structure revealed by the young populations is consistent with recent results using Gaia EDR3 astrometry and source lists based on near infrared photometry, showing the Local (Orion) arm to be at least 8 kpc long, and an outer arm consistent with what is seen in HI surveys, which seems to be a continuation of the Perseus arm into the third quadrant. Meanwhile, the subset of RGB stars with velocities clearly reveals the large scale kinematic signature of the bar in the inner disc, as well as evidence of

https://doi.org/10.1017/S1743921323002028 Published online by Cambridge University Press

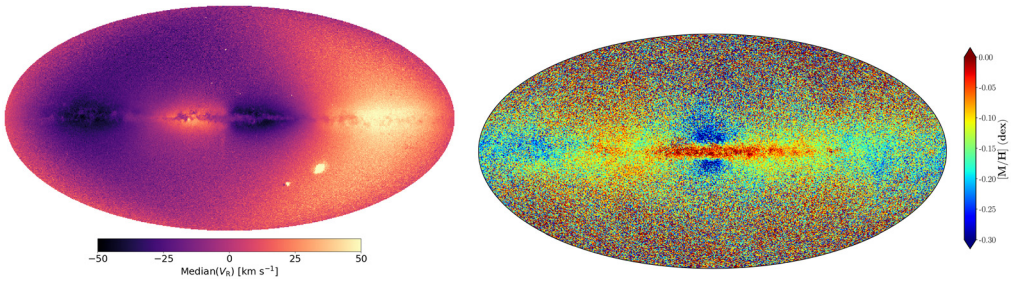

Figure 3. *Left*: Figure 5 from Katz *et al.* (2023) showing the sky map of the median radial velocity in each pixel with respect to the barycenter of the Solar system. The pattern of receding and approaching stars is the combination of the motion of the Sun and the galactic rotation. *Right*: Figure 2 from Gaia Collaboration, Recio-Blanco *et al.* (2023) showing the median of the stellar metallicity [M/H] in each pixel.

streaming motions in the outer disc that might be associated with spiral arms or bar resonances.

The all-sky Gaia chemical cartography (Fig. 3 right) allows a powerful and precise chemo-dynamical view of the Milky Way with unprecedented spatial coverage and statistical robustness (Gaia Collaboration, Recio-Blanco *et al.* 2023). The abundances have the required coverage and precision to unveil galaxy accretion debris and heated disc stars on halo orbits, and to allow the study of the chemo-dynamical properties of globular clusters. The abundance maps reveal the strong vertical symmetry of the Galaxy and the flared structure of the disc. There is a strong correlation of the kinematic disturbances of the disc with chemical patterns, both for young objects that trace the spiral arms and for older populations. Abundance elements (mainly iron-peak and α elements) trace the thin and thick disc properties in the solar cylinder. The abundances of open clusters, the largest sample analysed so far, show a steepening of the radial metallicity gradient with age, which is also observed in the young field population.

3.2. *Open clusters*

Simultaneous analysis of proper motions, parallaxes and photometry has allowed deep understanding of open clusters. The pre-*Gaia* samples (for instance Dias *et al.* (2002)) were revisited and enlarged. Hundreds of new open clusters have been identified in DR2 and EDR3 (for instance Castro-Ginard *et al.* (2022)). Young clusters and stellar associations show rich substructures with subpopulations of slightly different ages and kinematics unveiling the sequential process of formation line in Vela-Puppis (Cantat-Gaudin *et al.* 2019). Disruption, evaporation and streams have been also detected in many evolved clusters (Tarricq *et al.* 2022; Ratzenböck *et al.* 2020). All old clusters towards the center of the Galaxy reported in the pre-*Gaia* era, which should have been destroyed long time ago, show that they stars have incoherent proper motions and parallaxes, thus they are simply fortuitous projections on the sky and not physical groups (Cantat-Gaudin & Anders 2020). Young open clusters have been used to trace the spiral arms as seen in Fig. 4. They are in good agreement with other tracers like Cepheids, OB stars or masers.

3.3. *Acceleration of the Solar System*

The apparent proper motions of 1.2 million compact (QSO-like) extragalactic sources reveal a systematic pattern due to the acceleration of the Solar System barycentre with respect to the rest frame of the Universe (Gaia Collaboration, Klioner *et al.* 2021). The

https://doi.org/10.1017/S1743921323002028 Published online by Cambridge University Press

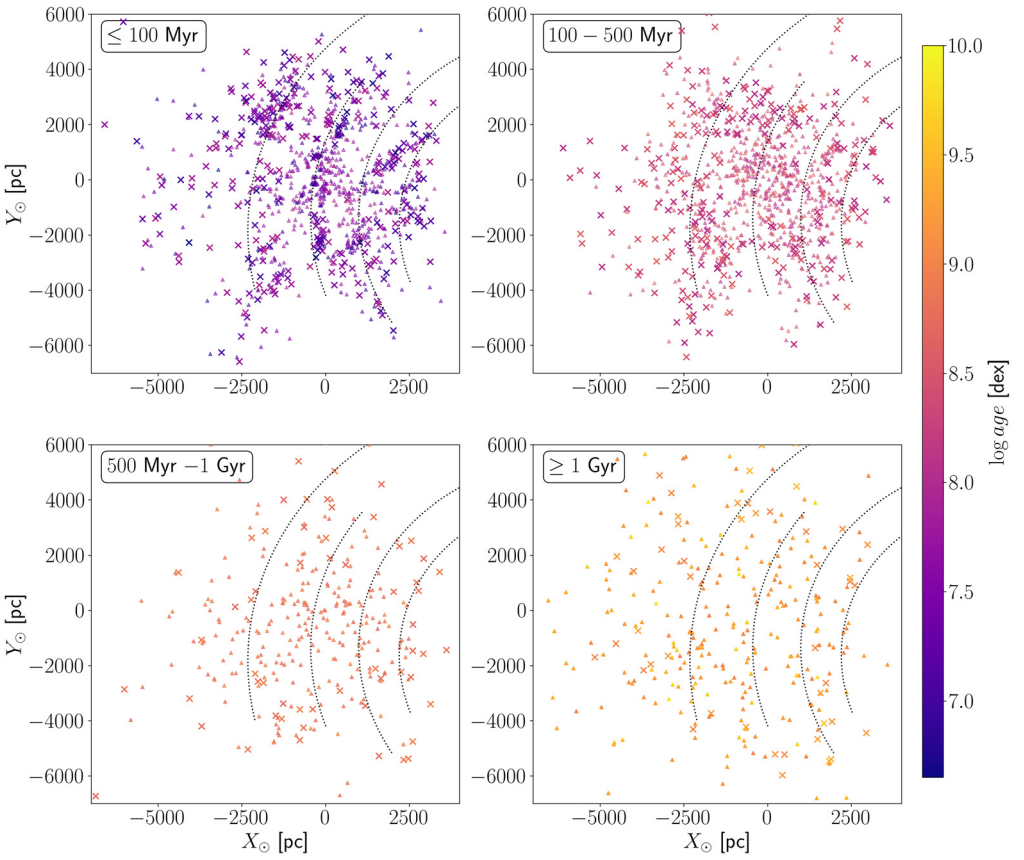

Figure 4. Figure 7 from Castro-Ginard *et al.* (2022). It shows the distribution of the new (crosses) and known (triangles) open clusters projected onto the Galactic plane for different age bins. The dotted lines show the spiral arms.

result is a proper motion amplitude of 5.05 ± 0.35 μas yr^{-1} that means an acceleration of $2.32 \pm 0.16 \cdot 10^{-10}$ m s^{-2}, in good agreement with the acceleration expected from current models of the Galactic gravitational potential. The accelerations point towards $\alpha = (269.1 \pm 5.4)^{\circ}$, $\delta = (-31.6 \pm 4.1)^{\circ}$, probably due to the presence of the Magellanic Clouds. We expect that future Gaia data releases will provide estimates of the acceleration with uncertainties substantially below 0.1μas yr^{-1}.

3.4. *Magellanic Clouds*

In spite that the *Gaia* proper motions and parallaxes for the Magellanic Clouds are at the limit of usability, radial and tangential velocity maps and global profiles have been derived (Gaia Collaboration, Luri *et al.* 2021) together with the spatial structure and motions in the central region, the bar, and the disc, providing new insights into features and kinematics. For the first time, the two planar components of the ordered and random motions are derived for multiple stellar evolutionary phases in a galactic disc outside the Milky Way, showing the differences between younger and older phases. Finally, *Gaia* data has allowed to resolve the Magellanic Bridge, and to trace the density and velocity flow of the stars from the SMC towards the LMC not only globally, but also separately for young and evolved populations.

https://doi.org/10.1017/S1743921323002028 Published online by Cambridge University Press

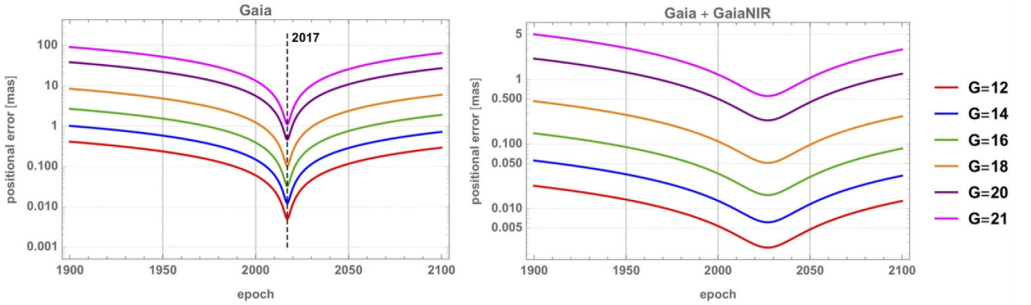

Figure 5. Figure 3 from Hobbs *et al.* (2023) showing the degradation over time of positions due to uncertainties on proper motions for *Gaia* (left) and a combination of *Gaia* and the future mission (right).

4. Near and far future

The satellite continues operating smoothly and ESA has approved the third extension of operations until 2025 where the cold gas to control the attitude will exhaust. We will have collected 10 years of science data that will overpass the initial expectations allowing better determination of all parameters and, more importantly, to detect of accelerations.

For the last quarter of 2023, DPAC foresees the publication of the Focused Product Release. It will include updated astrometry for Solar System objects, astrometry and photometry from engineering images for Omega Cen, the first results of quasars' environment analysis for gravitational lenses search, extended radial velocity epoch data for Long Period Variables, and diffuse interstellar bands from aggregated RVS spectra.

The results of the 5-yrs nominal mission duration, including both mean and epoch data, will constitute the fourth data release (DR4), and the complete data for the whole duration of the mission the fifth and final one (DR5), see https://www.cosmos.esa.int/web/gaia/release. DPAC is intensively working on the production of DR4 that is foreseen not before the end of 2025. DR5 is expected to be ready 5 years after the end of operations.

In spite of the revolution of *Gaia*, the optical regime limits the study of the Galaxy: the obscured regions by the dust are not directly accessible, and the observations of cold white dwarfs and brown dwarfs are limited, for instance. Current technology developments seem to promise competitive devices in the NIR for high precision astrometry. Therefore, the scientific community around *Gaia* has started to move towards the acquisition of all-sky optical and near infrared space astrometry in the future. This not only has a set of important science cases but also another key aspect: the combination of current positions obtained with *Gaia* combined with positions of a future mission will overcome the degradation of the positions due to the proper motions uncertainties, which would allow to maintain the realisation of the Celestial Reference Frame (see Fig. 5). Such a mission proposal (Hobbs *et al.* 2023) was submitted to ESA's call Voyage 2050, and the outcome of the evaluation is that space astrometry is one of the large themes in the Voyage 2050 framework, therefore providing excellent perspectives for the future.

Acknowledgements

This work has made use of results from the European Space Agency (ESA) space mission Gaia, the data from which were processed by the Gaia Data Processing and Analysis Consortium (DPAC). Funding for the DPAC has been provided by national institutions, in particular the institutions participating in the Gaia Multilateral Agreement. The Gaia mission website is http://www.cosmos.esa.int/gaia. The author is current member of

https://doi.org/10.1017/S1743921323002028 Published online by Cambridge University Press

the ESA Gaia mission team and of the Gaia DPAC. This work was (partially) supported by the Spanish MICIN/AEI/10.13039/501100011033 and by "ERDF A way of making Europe" by the "European Union" through grant PID2021-122842OB-C21, and the Institute of Cosmos Sciences University of Barcelona (ICCUB, Unidad de Excelencia 'María de Maeztu') through grant CEX2019-000918-M.

References

Antoja, T., Helmi, A., Romero-Gómez, M. *et al.* 2018, *Nature*, 561, 360
Cantat-Gaudin, T., Jordi, C., Wright, N. J. *et al.* 2019, *A&A*, 626, A17
Cantat-Gaudin, T., JAnders, F., 2020, *A&A*, 633, A99
Castro-Ginard, A., Jordi, C., Luri, X. *et al.* 2022, *A&A*, 661, A118
De Angeli, F., Weiler, M., Montegriffo, P., *et al.* 2023, *A&A*, in press, arXiv:2206.06143
Dias, W. S., Alessi, B. S., Moitinho, A., Lépine, J. R. D. 2002, *A&A*, 389, 871
Gaia Collaboration, Antoja, T., McMillan, P. J., *et al.* 2021, *A&A*, 649, A8
Gaia Collaboration, Brown, A. G. A., Vallenari, A., *et al.* 2016, *A&A*, 595, A2
Gaia Collaboration, Brown, A. G. A., Vallenari, A., *et al.* 2018, *A&A*, 616, A1
Gaia Collaboration, Brown, A. G. A., Vallenari, A., *et al.* 2021, *A&A*, 649, A1
Gaia Collaboration, Drimmel, R., Romero-Gómez, M., *et al.* 2023, *A&A*, in press, arXiv:2206.06207
Gaia Collaboration, Klioner, S. A., Mignard, F., *et al.* 2021, *A&A*, 649, A9
Gaia Collaboration, Luri, X., Chemin, L., *et al.* 2021, *A&A*, 649, A7
Gaia Collaboration, Prusti, T., de Bruijne, J. H. J., *et al.* 2016, *A&A*, 595, A1
Gaia Collaboration, Recio-Blanco, A., Kordopatis, G., *et al.* 2023, *A&A*, in press, arXiv:2206.05534
Gaia Collaboration, Vallenari, A., Brown, A. G. A., *et al.* 2023, *A&A*, in press, arXiv:2208.00211
Helmi, A., Babusiaux, C., Koppelman, H. H., *et al.* 2018, *Nature*, 563, 85
Hobbs, D., Brown, A., Høeg, E., *et al.* 2021, *Experimental Astronomy*, 51, 783
Katz, D., Sartoretti, P., Guerrier, A., *et al.* 2023, *A&A*, in press, arXiv:2206.05902
Lindegren, L., Klioner, S. A., Hernández, J., *et al.* 2021, *A&A*, 649, A2
Ratzenböck, S., Meingast, S., Alves, J., Möller, T., Bomze, I., 2020, *A&A*, 639, A64
Ramos, P., Antoja, T., Yuan, Z., *et al.* 2022, *A&A*, 666, A64
Ruiz-Lara, T., Gallart, C., Bernard, E. J., Cassisi, S., 2020, *Nature Astronomy*, 4, 965
Tarricq, Y., Soubiran, C., Casamiquela, L., *et al.* 2021, *A&A*, 659, A59